Chinese Chemical Letters 34 (2023) 107615

Contents lists available at ScienceDirect

Chinese Chemical Letters

journal homepage: www.elsevier.com/locate/cclet

Design and synthesis of liquid crystal copolyesters with high-frequency low dielectric loss and inherent flame retardancy

Shi-Yu Zhang, Teng Fu*, Yue Gong, De-Ming Guo, Xiu-Li Wang, Yu-Zhong Wang*

State Key Laboratory of Polymer Materials Engineering, The Collaborative Innovation Center for Eco-Friendly and Fire-Safety Polymeric Materials, National Engineering Laboratory of Eco-Friendly Polymeric Materials (Sichuan), College of Chemistry, Sichuan University, Chengdu 610064, China

ARTICLE INFO

Article history:
Received 22 April 2022
Revised 3 June 2022
Accepted 14 June 2022
Available online 18 June 2022

Keywords:
Liquid crystal polymer
Low dielectric loss
Low dielectric constant
Naphthalene structure
Flame retardant

ABSTRACT

Ultra-low dielectric loss (Df) and low dielectric constant (Dk) materials are urgently required in high-speed and large-capacity transmission, in which the wholly aromatic liquid crystal polymer (LCP) has gained attention due to its excellent dielectric properties. However, the relationship between molecular structure and dielectric properties is still not clear. In this study, two copolyesters containing phenyl or naphthyl structures are synthesized, as well as the effects of benzene and naphthalene mesogens on dielectric properties are investigated. The synthesized copolyesters containing naphthalene structure have good comprehensive properties with high thermal stability ($T_{5\%}$ = 479 °C and T_g = 195–216 °C), inherent flame retardance (LOI = 33.0–35.0 and UL-94 V-0 level at 0.8 mm), low Dk (2.9–3.0@10 GHz) and low Df (0.0027–0.0047@10 GHz). Naphthalene mesogen can reduce the dielectric loss more significantly than benzene at high frequency by reducing the density and mobility of polarizable groups, which leads to the effectively limited dipole polarization in copolyesters. Consequently, we proposed a new strategy for designing low Dk and low Df materials.

Explosive development for higher-speed and larger-capacity transmission in fields such as ultra-high-definition video transmission, internet of things, virtual reality, autonomous driving, proposes high-frequency communication above 6 GHz requirements [1]. As frequency increases, the signal transmission loss, closely related to the dielectric properties of the circuit substrate material, increases dramatically. The signal loss is proportional to frequency, dielectric loss (Df), and square root of dielectric constant (Dk) [2]. Thus, low Dk and ultra-low Df materials are strongly required for high quality transmission.

Traditional substrate materials such as epoxy resin, benzoxazine resin, and polyimide have high transmission losses in high-frequency regions [3]. Previous modification strategies (increasing pores or free volumes [3,4], introducing low-polarizable groups [5,6]) for reducing Dk and Df are still difficult to achieve the requirements of ultra-low loss (Df < 0.003) at high frequency [7]. Meanwhile, the thermal stability and flame retardancy of substrates cannot be ignored with the gradual development of high density and miniaturization of electronic devices. Therefore, a material with high-frequency low loss and meeting the comprehensive performance requirements of the circuit board should be urgently developed.

Recently, wholly aromatic liquid crystal polymers (LCP), composed of ester linkages and mesogenic units such as phenyl, naphthyl, and biphenyl, have attracted our attention due to their excellent low dielectric loss properties at high frequencies [8]. Prior researches have investigated the relationship between structure and properties (processing, thermal, and mechanical properties) of LCP materials [9,10]. Although LCP materials, such as the Vectra series launched by Celanese corporation, have been widely used as circuit board materials, few researchers have systematically explored the relationship between molecular structure and dielectric properties from the perspective of polymer structure design, causing unclear adjusting mechanism of dielectric properties for LCP materials.

In this work, poly(4-oxybenzoate-*co*-2,2-bis(4-oxyphenyl)propane terephthalate) (abbreviated as B-BPA) with phenyl structure as the main mesogenic unit and poly(6-oxy-2-naphthoate-*co*-2,2-bis(4-oxyphenyl)propane terephthalate) (abbreviated as N-BPA) with naphthyl as the main mesogenic unit are synthesized. Additionally, the kink bisphenol A structure is also introduced to control the melting point of copolyesters. The comprehensive properties of copolyesters are evaluated. Notably, the dielectric properties of copolyesters at low or high frequency are emphatically studied and the effect of mesogenic structure on

* Corresponding authors.
E-mail addresses: futeng@scu.edu.cn (T. Fu), yzwang@scu.edu.cn (Y.-Z. Wang).

https://doi.org/10.1016/j.cclet.2022.06.038
1001-8417/

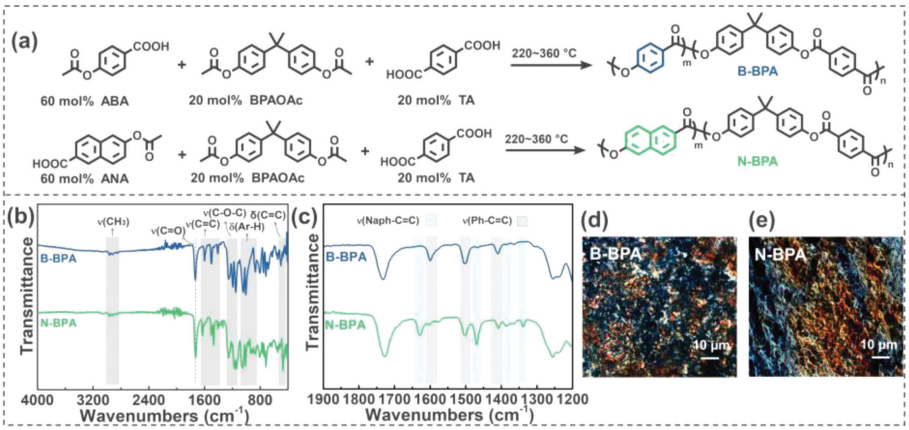

Fig. 1. (a) Synthetic routes of B-BPA and N-BPA copolyesters. (b) FTIR spectra of copolyesters. (c) Amplification of FTIR peaks between 1200 and 1900 cm^{-1}. (d) Polarizing micrographs of B-BPA and e) N-BPA at 320 °C.

dielectric properties is then investigated in detail, which provides a new strategy for designing low Dk and low Df materials.

As the synthetic routes shown in Fig. S1 (Supporting information), monomers such as 4-hydroxybenzoic acid (HBA), 6–hydroxy-2-naphthoic acid (HNA), and bisphenol A (BPA) are firstly acylated into 4-acetoxy benzoic acid (ABA), 6-acetoxy-2-naphthoic acid (ANA) and bisphenol A diacetate (BPAOAc) by an acylation reagent (acetic anhydride) to enhance the reactivity of monomers during the polymerization process [11]. The ^{1}H NMR spectra in Figs. S2a–c (Supporting information) confirm the chemical structure of acylation monomers. And the melting point (T_m) of ABA, ANA and BPAOAc are 188 °C, 223 °C and 93 °C, respectively, tested by the DSC. Then, as shown in Fig. 1a, melt polycondensation of ABA, BPAOAc, and terephthalic acid (TA) with a molar ratio of 60/20/20 is performed to prepare B-BPA copolyester composed of benzene rings, bisphenol A, and ester linkages. The N-BPA copolyester composed of naphthalene ring, benzene ring and bisphenol A with ester as linking groups is also prepared after replacing ABA with ANA.

The chemical structures of B-BPA and N-BPA copolyesters are confirmed by FTIR spectra in Fig. 1b. The characteristic absorption bands in 2964∼2850 cm^{-1} are assigned to the C−H stretching vibrations of aliphatic methyl groups. The absorption in 1732 and 1728 cm^{-1} is attributed to the C=O stretching vibrations of ester groups in B-BPA and N-BPA. Meanwhile, the ester groups also exhibit two bands in the range of 1256–1140 cm^{-1} due to the C−O−C stretching vibrations. The bands observed at 1603–1408 and 1629–1339 cm^{-1} are assigned to the aromatic C=C stretching vibrations of B-BPA and N-BPA, respectively. Comparing the peaks between 1630 and 1330 cm^{-1} in Fig. 1c, N-BPA has obvious C=C vibration peaks both in naphthalene rings (1629, 1470, 1386 and 1339 cm^{-1}) and benzene rings (1603, 1502 and 1408 cm^{-1}), while B-BPA only has C=C vibrations of benzene rings (1600, 1504 and 1409 cm^{-1}) [12,13], which further distinguishes the structures of B-BPA and N-BPA. In addition, the deformation vibrations of the alkane C−H at around 1364 cm^{-1}, the aromatic C−H at 1045–805 cm^{-1}, and the aromatic rings at 631–475 cm^{-1} are also observed. The absorption peaks mentioned above confirm the structure of B-BPA and N-BPA.

The inherent viscosities of B-BPA and N-BPA are determined by an Ubbelohde viscometer at 60 °C with pentafluorophenol as a solvent. The results show that the inherent viscosity of B-BPA is 0.7 dL/g, and N-BPA is 1.3 dL/g. Furthermore, we observed the thermotropic liquid-crystalline properties of B-BPA and N-BPA on the polarizing microscopy (POM) with a hot stage. As shown in Figs. 1d and e, both B-BPA and N-BPA exhibit a marbled texture under shearing at 320 °C, confirming the essence of nematic liquid crystal phase. The above results illustrate the successful synthesis of B-BPA and N-BPA wholly aromatic liquid crystal copolyesters.

Thermal transition behaviors of B-BPA and N-BPA are further investigated by a differential scanning calorimeter (DSC). It is found that B-BPA shows a glass transition at 195 °C (glass transition temperature, T_g) and a crystalline to nematic phase transition at 248 °C (nematic phase transition temperature, T_N) according to the second heating curves in Fig. 2a. Meanwhile, a nematic to crystalline phase transition is also observed at 232 °C (crystallization temperature, T_c) during the cooling process with a crystallization enthalpy (ΔH_c) of 6.0 J/g (Fig. 2b). Compared with B-BPA, N-BPA has a higher T_g (216 °C) and higher T_c (295 °C), but shows significantly reduced ΔH_c (0.1 J/g) and no liquid crystal transition peak. The X-ray diffraction (XRD) patterns in Fig. 2c are used to analyze this phenomenon. The crystallinity (X_c) of B-BPA and N-BPA fitted by Jade software is 11.7% and 3.3%. Obviously, the introduction of naphthalene ring structure makes N-BPA low crystallinity, so that no liquid crystal transition is observed and the crystallization peak intensity is weakened.

The thermal stability of B-BPA and N-BPA is conducted through thermogravimetry analysis (TGA). As shown in Fig. 2d, both B-BPA and N-BPA have excellent thermal stability, with their 5 wt% weight loss temperatures ($T_{5\%}$) being 479 °C. The maximum mass loss rate temperature (T_{max}) of B-BPA is 500 °C, while that of N-BPA is slightly higher at 506 °C. In addition, the char residue (CR) at 700 °C of B-BPA and N-BPA are 41.3 wt% and 47.6 wt%. The high CR of the two copolyesters means that their fully aromatic structure can promote the formation of residual char during thermal decomposition, which is beneficial to flame retardancy. The higher residual mass of N-BPA also indicates that naphthalene structure can endow the polymer with better char-forming ability compared with benzene structure.

The water absorption and Z-axis thermal expansion coefficient (CTE_Z) of substrate materials are the key parameters in high-frequency applications. Low water absorption is beneficial to ensure the stability of the dielectric properties of materials in the environment. Fig. 2e and Table S1 (Supporting information) show the water absorption rate of B-BPA and N-BPA after being placed in water for 3 days. Compared with polyimide (3.01%) [14], B-BPA and N-BPA have an ultra-low water absorption rate of 0.47% and 0.33%, respectively, which is conducive to its high frequency application. In addition, the CTE_Z of B-BPA and N-BPA shown in Fig. 2f are 59 and 72 ppm/K, respectively. The N-BPA shows a higher CTE_Z than B-BPA, which can be attributed to the introduction of crankshaft naphthalene structure, leading to the increased chain spacing and weakened intermolecular forces.

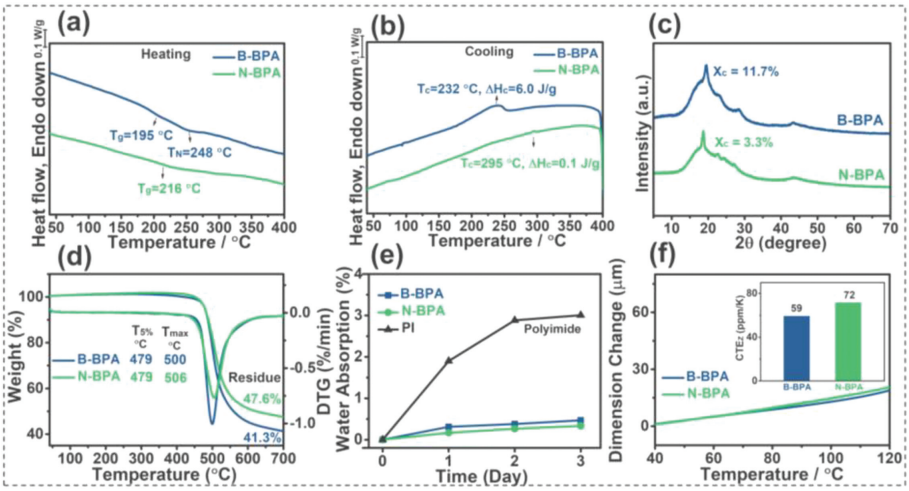

Fig. 2. (a) The seconding heating and (b) the cooling curves in DSC tests. (c) XRD patterns. (d) Thermogravimetric curves under N_2 atmosphere. (e) The water absorption rate after being placed in water for 3 days. (f) The CTEZ of B-BPA and N-BPA copolyesters.

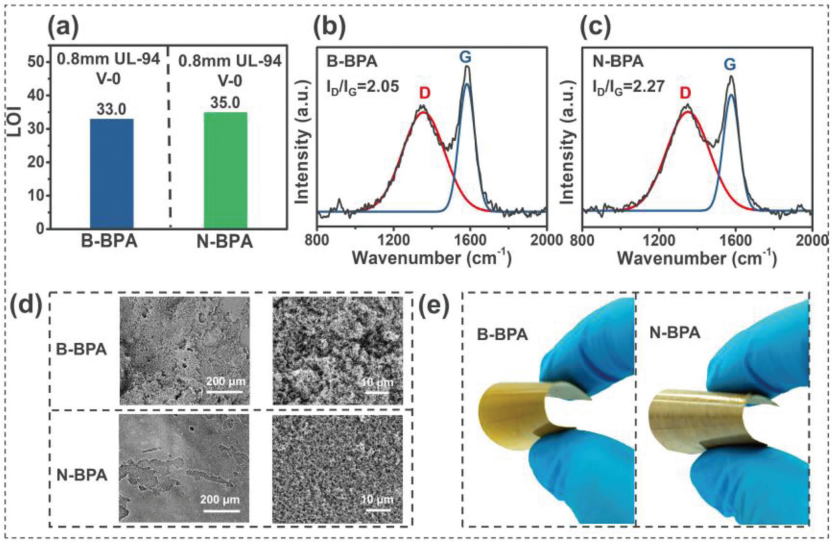

Fig. 3. (a) Limiting oxygen index and vertical burning test results. (b) The Raman spectra of the char residue of B-BPA and (c) N-BPA. (d) The SEM images of the char residue surface of B-BPA and N-BPA. (e) Flexible films images prepared by the hot-pressing procedure.

High flame retardancy of substrate material is necessary to ensure the safety of electrical circuits. The flame-retardant properties are firstly evaluated by limiting oxygen index (LOI). The LOI refers to the minimum oxygen concentration required to sustain burning. Generally, materials with LOI values above 26 are considered to be highly flame retardant [15]. As shown in Fig. 3a, the LOI values of B-BPA and N-BPA are 33.0 and 35.0, respectively. In addition, the UL-94 vertical burning test is another important measurement to evaluate the fire safety of materials. Generally, few polymers can reach a UL-94 V-0 rating at 1.5 mm thickness without adding flame retardant [16]. Notably, both B-BPA and N-BPA achieve the V-0 level at 0.8 mm thickness with no droplets produced, in which they can self-extinguish after two ignitions with a total burning time of less than 10 s. These results indicate that both copolyesters exhibit excellent intrinsic flame retardance, and N-BPA is slightly better than B-BPA.

Moreover, the Raman spectroscope and scanning electron microscope (SEM) tests are used to explain the flame retardant mechanism. The char of B-BPA and N-BPA has two characteristic absorption peaks near 1360 cm^{-1} (D-band) and 1580 cm^{-1} (G-band), which represents the structure of defective graphitized carbon and sp^2 hybridized carbon, respectively [17]. A larger peak area ratio of the D and G band (I_D/I_G) means a smaller crystallite structure and a denser char layer. In Figs. 3b and c, compared with B-BPA whose I_D/I_G is 2.05, the N-BPA has a higher I_D/I_G (2.27), indicating that the naphthalene structure can reduce the crystallite size and promote the formation of the denser char layer. The SEM images in Fig. 3d also confirmed this result. N-BPA obviously possesses a denser char layer compared to B-BPA. The dense and stable char layer prevents oxygen ingress and heat transfer [18], thus resulting in an improved flame retardancy of N-BPA. Furthermore, in Fig. 3e, B-BPA and N-BPA copolyesters not only have the above-mentioned excellent thermal and flame retardant properties but also have good processability, which can be prepared into flexible films with smooth surfaces using a simple hot-pressing procedure.

Then, we focus on the effect of the mesogenic structure on the dielectric properties. The broadband dielectric behavior in the low-frequency region (1–10^6 Hz) enables to gain a wealth of dynamic information on the dipoles depending on the details of the molecular structure [19]. Five types of polarization mechanisms exist in polymers including electronic, atomic, dipolar, ionic, and interfacial polarization [20,21]. For most polymeric dielectrics, dipolar polar-

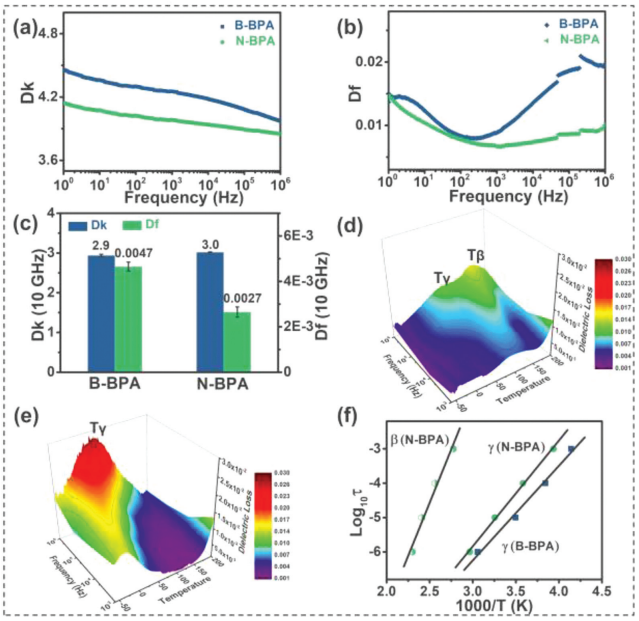

Fig. 4. (a) Dk and (b) Df of B-BPA and N-BPA copolyesters over a frequency range of 1–10^6 Hz. (c) Dk and Df of B-BPA and N-BPA with different HNA content at 10 GHz. (d) The dielectric relaxation spectra of N-BPA and (e) B-BPA with the various temperature at 10^3–10^6 Hz. (f) The Arrhenius plots of logτ *versus* T^{-1}.

ization which occurs in the frequency range from 1 kHz to tens of MHz is primarily important and dominates the dielectric behavior [21].

In Fig. 4a, compared with B-BPA whose Dk is 4.0–4.5 at frequencies from 1–10^6 Hz, N-BPA containing naphthalene structures has a lower Dk (3.9–4.1). In frequency versus Df curves (Fig. 4b), the loss peak is caused by the delay of polarization with respect to a changing electric field. The peak located at 1–10^3 Hz originates from interfacial polarization, while the other peak over 10^3–10^6 Hz is assigned to the dipole polarization relaxation [22,23]. It can be found that the dipole relaxation peak of naphthalene-containing N-BPA in 10^3–10^6 Hz is weakened with a significantly lower loss peak than B-BPA. These results indicate that the dipole polarization loss can be effectively reduced by the naphthyl mesogen rather than phenyl mesogen. Moreover, the Dk and Df at 10 GHz are further measured according to the standard IEC 61,189–2–721:2015. Fig. 4c shows no significant difference in Dk between B-BPA (2.9) and N-BPA (3.0). On the contrary, the Df of N-BPA (0.0027) exhibiting a much lower value than that of B-BPA (0.0047), satisfies the ultra-low Df requirement (<0.003) [7] in high-frequency communication.

Next, the regulation mechanisms of naphthalene structure on dielectric properties are discussed. First, the interlayer distances of B-BPA and N-BPA are investigated by XRD. As shown in Fig. S3 (Supporting information), compared with B-BPA with a *d*-spacing of 4.54 Å, the N-BPA with naphthalene structure has increased to 4.75 Å. According to the XRD and DSC analysis mentioned above, the introduction of naphthalene structure reduces the crystallinity of the material, and occurs a greater distorted O′ orthorhombic phase (corresponding to the diffraction peak at 24.6°) in crystal structure of N-BPX [24]. Thus, the increase of *d*-spacing can be attributed to the disturbed chain regularity caused by crankshaft naphthalene structure. The increased *d*-spacing of polymer is considered to affect the chain packing and density, resulting in a reduced density of polarizable group [25]. According to the Clausius-Mossotti equation, lower dipole density is beneficial to reduce Dk [26]. Thus, the lower Dk of N-BPA than B-BPA in the broadband dielectric test is attributed to the enhanced interlayer distance by naphthalene structure. However, the increased d-spacing does not bring a significant effect on the Dk of B-BPA and N-BPA at 10 GHz, due to the insufficient polarization of dipoles at high frequencies weakening the effect of dipole density on Dk.

In the dielectric loss aspect, the Df is caused by dipolar relaxation. Especially, dipolar relaxation of B-BPA and N-BPA copolyesters is mainly due to torsional vibrations of ester carbonyl (C=O) in polymer chains [27]. Therefore, in order to investigate the localized movement of carbonyl groups, the dielectric relaxation spectra are measured at −60~200 °C in the frequency range that produces dipole polarization (10^3–10^6 Hz). As shown in Fig. 4d and Table S2 (Supporting information), N-BPA exhibit two secondary relaxation processes. One is the γ relaxation that occurs at lower temperatures (−19~64 °C), which is assigned to the localized motion of carbonyl groups linked to phenyl groups. Another is the β relaxation in the higher temperature at 87–162 °C, originated from the localized motion of carbonyl groups linked to naphthyl units [23–28]. Comparatively, in Fig. 4e, B-BPA only exhibits a single relaxation process at −32~54 °C, which is produced by the localized motion of carbonyl groups linked to phenyl group [23], similar to the γ relaxation of *N*-BPA. The γ relaxation temperature (T_γ) is significantly lower than the β relaxation temperature (T_β), suggesting that the carbonyl groups linked to naphthyl structure rotate more difficultly than to phenyl units. And the T_γ below or close to room temperature also indicates that all phenyl-linked carbonyl groups are the main source of polarization loss at normal operating temperatures. Comparing the dielectric spectra of the two copolyesters in Fig. S4 (Supporting information), the peak intensity of γ relaxation of naphthalene-containing N-BPA is significantly lower than that of B-BPA, and is accompanied by the appearance of higher temperature β relaxation. This means that the number of γ relaxed carbonyl groups are reduced and more carbonyl groups are fixed at β relaxation that hardly produces dielectric loss at room temperature when naphthalene as the main mesogenic structure.

The activation energy of ester carbonyl groups connected with different mesogenic units are further calculated according to the Arrhenius plots in Fig. 4f. The rotational activation energy for phenyl linked carbonyl groups in B-BPA is 52.7 kJ/mol, and for phenyl or naphthyl linked carbonyl groups in N-BPA is 58.9 and 118.5 kJ/mol, respectively. Obviously, compared with B-BPA, the dipole rotation in N-BPA needs to overcome a higher barrier, making it more difficult for the dipole to move, thus inhibiting dipole polarization and reducing dielectric loss.

In summary, we explore the effect of benzene and naphthalene structures on the Dk and Df of LCP, and analyze the mechanism of these mesogenic structures on dielectric properties in detail. It is found that the introduction of naphthalene structure reduces the density and mobility of polarizable groups, which leads to the effectively limited dipole polarization in copolyesters. Therefore, the dielectric loss of N-BPA (0.0027) dominated by naphthyl mesogen is 43% lower than that of B-BPA (0.0047) dominated by phenyl mesogen under 10 GHz. Besides, the N-BPA copolyester also has good comprehensive properties (high thermal stability and inherent flame-retardance), demonstrating the potential application on high frequency electronic substrates.

Declaration of competing interest

The authors declare no competing financial interest.

Acknowledgments

This work was financially supported by the National Natural Science Foundation of China (Nos. 51991351 and 51991350), the

Fundamental Research Funds for the Central Universities, the 111 Project (No. B20001), and the Sichuan Science and Technology Program (No. 2020YFH0016)

Supplementary materials

Supplementary material associated with this article can be found, in the online version, at doi:10.1016/j.cclet.2022.06.038.

References

[1] I. Nishimura, S. Fujitomi, Y. Yamashita, N. Kawashima, N. Miyaki, IEEE Proc. Electron. Compon. Technol. Conf. (2020) 641–646.
[2] Y.H. Kim, Y.W. Lim, Y.H. Kim, B.S. Bae, ACS Appl. Mater. Interfaces 8 (2016) 8335–8340.
[3] J. Chen, M. Zeng, Z. Feng, et al., ACS Appl. Polym. Mater. 1 (2019) 625–630.
[4] X. Li, T. Liu, Y. Jiao, et al., Chem. Eng. J. 359 (2019) 641–651.
[5] C.C. Kuo, Y.C. Lin, Y.C. Chen, et al., ACS Appl. Polym. Mater. 3 (2020) 362–371.
[6] J. Duan, C. Mei, W. Wu, et al., Macromolecules 54 (2021) 6947–6955.
[7] J. Guo, H. Wang, C. Zhang, Q. Zhang, H. Yang, Polymers 12 (2020) 1875.
[8] Y. Ji, Y. Bai, X.B. Liu, K. Jia, Adv. Ind. Eng. Polym. Res. 3 (2020) 160–174.
[9] V.K. Thakur, M.R. Kessler, Liquid Crystalline Polymers: Volume 1-Structure and Chemistry, Springer, Switzerland, 2016.
[10] H.N. Yoon, L.F. Charbonneau, G.W. Calundann, Adv. Mater. 4 (1992) 206–214.
[11] A. Buyle Padias, H.K. Hall Jr, Polymers 3 (2011) 833–845.
[12] A. Pirnia, C.S.P. Sung, Macromolecules 21 (1988) 2699–2706.
[13] I. Ouchi, M. Hosoi, S. Shimotsuma, J. Appl. Polym. Sci. 21 (1977) 3445–3456.
[14] B.X. Du, Z.Y. He, Q. Du, Y.G. Guo, IEEE Trans. Dielectr. Electr. Insul. 23 (2016) 134–141.
[15] J.W. Long, X.H. Shi, B.W. Liu, et al., Acta Polym. Sin. 51 (2020) 681–686.
[16] P. Patel, T.R. Hull, C. Moffatt, Fire Mater. 36 (2012) 185–201.
[17] A. Sadezky, H. Muckenhuber, H. Grothe, R. Niessner, U. Pöschl, Carbon 43 (2005) 1731–1742.
[18] B.W. Liu, H.B. Zhao, Y.Z. Wang, Adv. Mater. 34 (2021) 2107905.
[19] F. Kremer, A. Schönhals, Broadband Dielectric Spectroscopy, Springer Science & Business Media, Berlin, 2002.
[20] L. Zhu, Q. Wang, Macromolecules 45 (2012) 2937–2954.
[21] B. Wang, W. Huang, L. Chi, et al., Chem. Rev. 118 (2018) 5690–5754.
[22] B. Wang, L. Liu, G. Liang, L. Yuan, A. Gu, J. Mater. Chem. A 3 (2015) 23162–23169.
[23] D.S. Kalika, D.Y. Yoon, Macromolecules 24 (1991) 3404–3412.
[24] D.J. Wilson, C. Vonk, A. Windle, Polymer 34 (1993) 227–237.
[25] C. Qian, R. Bei, T. Zhu, et al., Macromolecules 52 (2019) 4601–4609.
[26] Z. Ahmad, Polymer Dielectric Materials, IntechOpen, London, 2012.
[27] M.G. Saphiannikova, N.V. Lukasheva, A.A. Darinskii, Y.Y. Gotlib, J. Brickmann, Macromolecules 33 (2000) 606–612.
[28] T.T. Hsieh, C. Tiu, G.P. Simon, Polymer 41 (2000) 4737–4742.